

FREQUENCY CALIBRATIONS WITH CONVENTIONAL TIME INTERVAL COUNTERS VIA GPS TRACEABILITY

Juan José González de la Rosa, I. Lloret

Univ. Cádiz. Research Group TIC168, EPSA. Av. Ramón Puyol S/N. E-11202-Algeciras-Cádiz-Spain,

Carlos García Puntonet, J. M. Górriz

Univ. Granada. Dept. ATC, ESII. Periodista Daniel Saucedo. E-18071-Granada-Spain

A. Moreno, M. Liñán and V. Pallarés

Univ. Córdoba. Electronics Area, Campus Rabanales. A. Einstein C-2. E-14071-Córdoba-Spain

Keywords: AVAR, frequency calibrations, GPS receiver, MVAR, noise processes, traceable standard, type B uncertainty, uncertainty calculations.

Abstract: Calculation of the uncertainty in traceable frequency calibrations is detailed using low cost instruments, partially characterized. Contributions to the standard uncertainty have been obtained under the assumption of uniform probability density function of errors. Short term instability has been studied using non-classical statistics. A thorough study of the noise processes characterization is made with simulated data by means of our variance estimators. The experiment is thought for frequencies close to 1 Hz.

1 INTRODUCTION

Time interval counters (TICs) and GPS receivers are widely used in traceable frequency calibrations. A transfer standard receives a signal that has a cesium oscillator as source (Lombardi, 1996). This signal delivers a cesium derived frequency to the user, who is benefited as not all laboratories can afford a cesium (Lombardi, 1996). These instruments differ in specifications and details regarding the time base, the main gate and the counting assembly. Furthermore, manufacturers tend to omit the conditions under these specifications have been provided or measured.

The purpose of this paper is twofold. First we detail the uncertainty calculations and the magnitudes which contribute to the sensitivity coefficients in the uncertainty propagation. Second, we show how to deal with practical situations which involve incomplete specifications. Experimental results are obtained under the assumption of white noise as the main cause of short term instability, which is corroborated later by means of the non-classical statistics AVAR¹ and MVAR². A prior analysis of noise processes is made to show short term instability characterization, by analyzing the slopes of the AVAR and MVAR in the log-log curves. Noise time series have

been simulated and estimators of the variances have been programmed with the aim of having a thorough vision of the time-domain slopes when compared to former works: (Howe et al., 1999), (Allan, 1987), (Rutman and Walls, 1991), (Vernotte, 1993), (Vig, 2001).

The paper is structured as follows: in Section 2 we review the oscillators independent noise processes and the methods used to identify them; Section 3 shows the details concerning uncertainty calculations. Experiments are drawn in Section 4, and conclusions explained in Section 5.

2 CLASSICAL NOISE MODELS

2.1 Characterizing Instabilities

The instantaneous output voltage of an oscillator can be expressed as:

$$v(t) = [V_o + \varepsilon(t)] \sin [2\pi\nu_0 t + \phi(t)], \quad (1)$$

where V_o is the nominal peak voltage amplitude, $\varepsilon(t)$ is the deviation from the nominal amplitude, ν_0 is the name-plate frequency, and $\phi(t)$ is the phase deviation from the ideal phase $2\pi\nu_0 t$. Changes in the peak value of the signal is the amplitude instability. Fluctuations in the zero crossings of the voltage is the phase instability. The so-called frequency instability is depicted

¹Allan variance or two-sample Allan variance

²Modified Allan variance

by the fluctuations in the period of the voltage. The situation was depicted in (Vig, 2001) and (de la Rosa et al., 2005).

The short-term stability measures most frequently found on oscillator specification sheets is the two-sample deviation, also called Allan deviation, $\sigma_y^2(\tau)$ (Howe et al., 1999), (Vig, 2001).

Classical variance in non-stationary noise processes doesn't converge to concrete values. It diverges for some noise processes (de la Rosa et al., 2005). This is the reason whereby non-classical statistics are used to characterize short term instability. AVAR and MVAR have proven their adequacy in characterizing frequency phase and instabilities. These easy-to-compute variances converge for all noise processes observed in precision frequency sources, have a straightforward relationship to power law spectral density of noise processes, and are faster and more accurate than the FFT (Lesage and Ayi, 1984).

The estimates of AVAR and MVAR for a given calibration time τ for a m -data series of phase differences, x , are given by equations 2 and 3, (Greenhall, 1988):

$$\begin{aligned} AVAR \equiv \sigma_y^2(\tau, m) &= \frac{1}{2(m-1)} \sum_{j=2}^m (\bar{y}_j - \bar{y}_{j-1})^2 \\ &= \frac{1}{2\tau^2(m-1)} \sum_{j=2}^m [\Delta_\tau^2 x(j\tau)]^2 \end{aligned} \quad (2)$$

$$MVAR \equiv \frac{1}{2\tau^2} \langle \Delta_\tau^2 \bar{x} \rangle^2, \quad (3)$$

where the bar over x denotes the average in the time interval τ (averaging time), and $\Delta_\tau^2 x = x_{i+2} - 2x_{i+1} + x_i$, is the so called second difference of x . The fractional frequency deviation is the relative phase difference in an interval τ . It is defined by equation 4:

$$\bar{y} = \frac{1}{\tau} \int_{t-\tau}^t y(s) ds = \frac{x(t) - x(t-\tau)}{\tau} = \frac{\Delta_\tau x(t)}{\tau}. \quad (4)$$

Non-classical statistics estimators, defined above, in equations 2 and 3, for non-stationary series characterization, give an average dispersion of the fractional frequency deviation due to the noise processes coupled to the oscillator. As a consequence time domain instability (two-sample variance) is related to the noise spectral density via (Rutman and Walls, 1991):

$$\sigma_y^2(\tau) = \frac{2}{(\pi\nu_0\tau)^2} \int_0^{f_h} S_\phi(f) \sin^4(\pi f\tau) df, \quad (5)$$

where ν_0 is the carrier frequency and f is the Fourier frequency (the variable), and f_h is the band-width of

the measurement system. $S_\phi(f)$ is the spectral density of phase deviations, which is in turn related to the spectral density of fractional frequency deviations by (Rutman and Walls, 1991):

$$S_\phi(f) = \frac{\nu_0^2}{f^2} S_y(f), \quad (6)$$

The classical power-law noise model is a sum of the five common spectral densities. The model can be described by the one-sided phase spectral density $S_\phi(f)$ via (IEE, 1988), (Greenhall, 1988):

$$S_\phi(f) = \frac{\nu_0^2}{f^2} \sum_{\alpha=-2}^2 h_\alpha f^\alpha = \nu_0^2 \sum_{\beta=0}^4 h_\beta f^\beta, \quad (7)$$

for $0 \leq f \leq f_h$. Where, again, f_h is the high-frequency cut-off of the measurement system (the band-width); h_α and h_β are constants which represent, respectively, the independent characteristic models of oscillator frequency and phase noise (Allan, 1987), (IEE, 1988), (Greenhall, 1988).

For integer values (the most common case) we have the following approximate expression:

$$\sigma_y(\tau) \sim \tau^{\mu/2}, \quad (8)$$

where $\mu = -\alpha - 1$, for $-3 \leq \alpha \leq 1$; and $\mu \approx -2$ for $\alpha \geq 1$. In the case of the modified Allan variance, the time-domain instability can be approximated via:

$$Mod\sigma_y(\tau) \sim \tau^{\mu'} \quad (9)$$

Hereinafter we use expressions 8 and 9 for analyzing noise in these work.

2.2 Time Domain Stability Characterization Curves

Equations 8 and 9 are used to make the graphical representation of $\sigma_y(\tau)$ vs. τ , and lets us infer the noise processes which causes frequency instability by means of measuring the slope in a log-log graph (Rutman and Walls, 1991). These functional characteristics of the independent processes are widely used in modelling frequency instability of oscillators. Table 1 shows the experimental criteria adopted in the main references. In the second column or MVAR we have picked up two different criteria according to the references (Rutman and Walls, 1991) and (Lesage and Ayi, 1984), respectively. We have kept the notation in the works (Rutman and Walls, 1991) and (Lesage and Ayi, 1984) for $\mu/2$ and μ' , respectively.

The five noise processes have been modelled and VAR and MVAR have been calculated. Hereinafter we show the simulation results of the time-series and their associated VAR and MVAR graphs. From this simulations we adopt the criteria depicted in the second column of MVAR in table 1. Figures 1-5 show

Table 1: Noise processes characterized by the time and frequency domain slopes. Up to bottom: random walk frequency modulation, flicker frequency modulation, white frequency modulation, flicker phase modulation, white phase modulation.

		AVAR	MVAR
$S_y(f)$	$S_\phi(f)$	$\sigma_y(\tau) \sim \tau ^{\frac{\mu}{2}}$	$\sigma_y(\tau) \sim \tau ^{\mu'}$
α	$\beta = \alpha - 2$	$\frac{\mu}{2}$	μ'
-2	-4	0.5	1 (0.5)
-1	-3	0	0 (0)
0	-2	-0.5	-1 (-0.5)
1	-1	-1	-2 (-1)
2	0	-1	-3 (-1.5)

the results. Each sequence contains 4096 points for a time resolution of $\tau = 10^{-4}$ s. Allan deviation curves have been depicted for averaging times $\tau = n \times \tau_0$, with $n \in [1, 500]$.

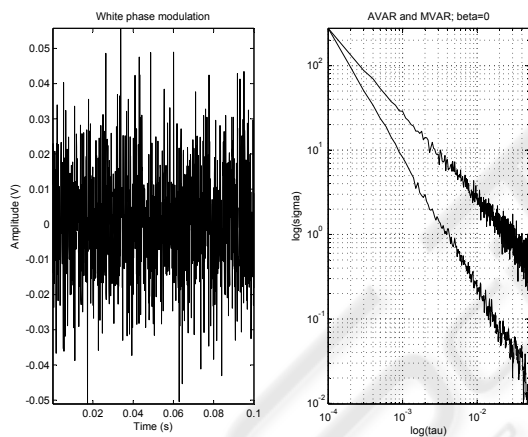


Figure 1: Characterization of a noise process corresponding to $\beta = 0$.

In practice, two or more noise processes simultaneously affect clocks performance. In this cases instability of the device under test is explained away through the behaviour of the upper enveloping curve. If the individual variance curves cross each other, it is possible to see the slope changes in the variance curve, for a time-series which includes several types of noise(Vernotte, 1993). This situation is shown in figures 6 and 7.

In figure 6, the individual variance curves cross. So the enveloping curve characterizes the short-term instability. By the contrary, in figure 7 the $\beta = 0$ noise processes has a variance greater than the $\beta = -4$ perturbation. In this case the enveloping curve is the first (upper) AVAR curve.

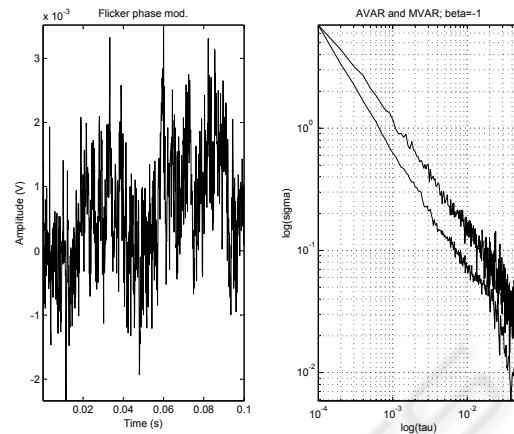


Figure 2: Characterization of a noise process corresponding to $\beta = -1$.

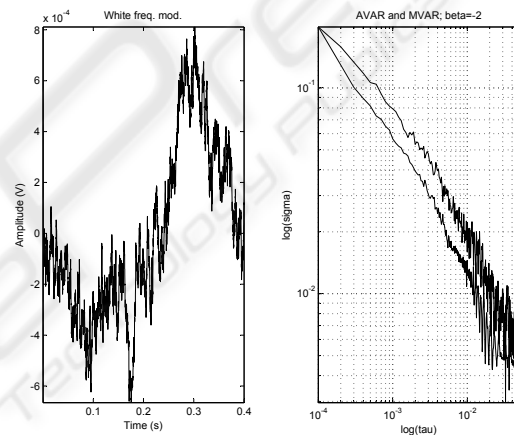


Figure 3: Characterization of a noise process corresponding to $\beta = -2$.

3 UNCERTAINTY PROPAGATION USING A REFERENCE SIGNAL OF 1 PPS

3.1 Sensitivity Coefficients in the Measurement System

In calibration we usually deal with a measurand, Z , which is the particular quantity subject to the measurement and is considered as the output of the measurement system. This quantity depends upon a set of input random variables X_i according to a functional relationship given by a function f , representing the procedure of the measurement and the method of evaluation (Force, 1999):

$$Z = f(X_1, X_2, \dots, X_N) \tag{10}$$

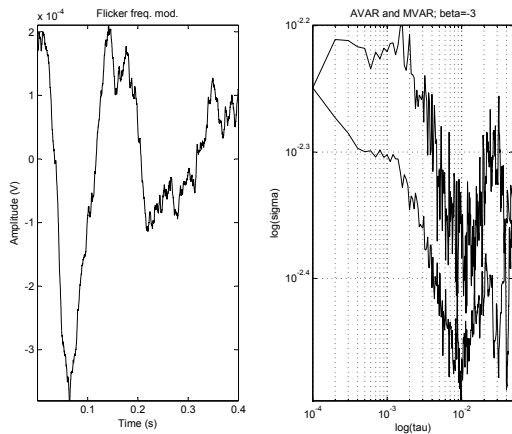


Figure 4: Characterization of a noise process corresponding to $\beta = -3$.

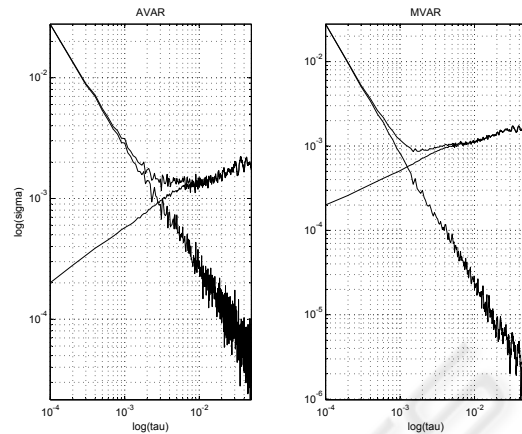


Figure 6: Noise processes corresponding to $\beta = 0$ and $\beta = -4$. Situation of changing slope.

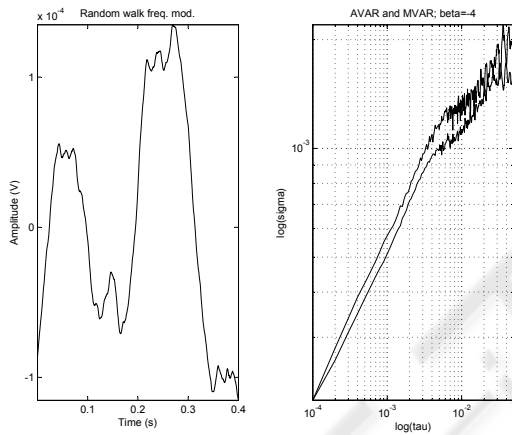


Figure 5: Characterization of a noise process corresponding to $\beta = -4$.

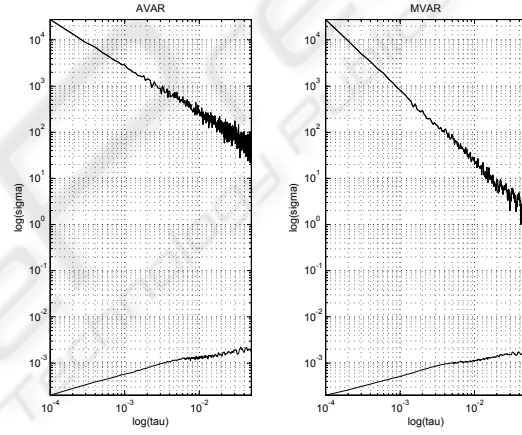


Figure 7: Noise processes corresponding to $\beta = 0$ and $\beta = -4$. The upper noise process is the enveloping curve.

An estimate of the measurand, denoted by z , is obtained from equation 10 using input estimates x_i :

$$z = f(x_1, x_2, \dots, x_N) \quad (11)$$

The standard uncertainty associated with that estimate $u(z)$, depends on the particular uncertainties of the input quantities $u(x_i)$. For uncorrelated inputs the square of the standard uncertainty of the output estimate is given by:

$$u^2(z) = \sum_{i=1}^N u_i^2(z), \quad (12)$$

where the individual contributions in equation 12 are obtained through the sensitivity coefficients c_i via:

$$u_i(z) = c_i u(x_i), \quad c_i = \left[\frac{\partial f}{\partial X_i} \right]_{x_i} \quad (13)$$

3.2 Types of Uncertainty for the Input Estimates

The Type A evaluation of standard uncertainty is the method which considers the statistical analysis of a series of observations. The standard uncertainty is the experimental standard deviation of the mean, which in turn results from a regression analysis. By the contrary, the Type B method is based on scientific knowledge (Force, 1999). The standard uncertainty of one input estimate $u(x_i)$, evaluated via the Type B method, comprises all the information related to the variability of the measurand X_i . This variability can fall into the following six categories, described in (de la Rosa et al., 2005).

Insight and general knowledge are the sources of information for a Type B evaluation of standard uncertainty. In this paper no probability distribution is provided in the data sheets for the quantities X_i . Only

upper and lower limits can be estimated for the values of the quantities in the manufacturer's specifications. So a rectangular probability distribution is a reasonable description of one's inadequate knowledge about an input quantity in absence of any other information apart from its limits of variability.

3.3 The Measurand in Traceable Frequency Characterization

In traceable frequency calibrations the expression for the measurand f_{meas} is given by:

$$f_{meas} = \left[\frac{f_{REF}}{1 \pm f_{REF} \frac{\Delta x}{\tau}} \right]_{f_{REF}, \Delta x, \tau} \quad (14)$$

where f_{REF} is the reference (1 pps), Δx represents the phase shift between the source under test and the reference, and τ is the averaging time or the calibration period of the measurement system. Expression 14 is evaluated in the averaged phase shift during the calibration period. For a zero phase shift or an infinity averaging time, we have the ideal case ($f_{meas} = f_{REF}$).

Using equations 12, 13 and 14, the uncertainty of the frequency is obtained from equation 15:

$$u^2(f_{meas}) = \left(1 - f_{REF} \frac{\Delta x}{\tau} \right)^{-4} \times [u^2(f_{REF}) + u^2(\Delta x) + u^2(\tau)] \quad (15)$$

Sensitivity coefficients in expressions 12 and 13 determine the contributions of the type B uncertainty, which is associated to the instrument specifications.

4 EXPERIMENTAL RESULTS

4.1 Uncertainty Calculations

A high resolution function generator is chosen as device under test. It is set up to deliver a 1.1 Hz TTL signal. The experimental arrangement is depicted in figure 8. The measurement system comprises a TIC³, a GPS receiver and the frequency source under test. These instruments have been connected via GPIB to the computer. Data points are captured every 1 s.

Figure 9 shows the signals involved in the measurement process. Each measurement cycle corresponds to 1 s. The bottom graph corresponds to the instantaneous phase-deviation series, which comprises $m = 898$ data. These data are the result of filtering the spiky time-series of phase differences, and are

³Time Interval Counter

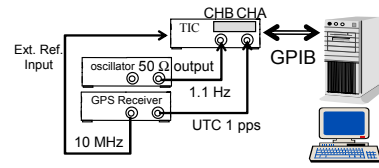


Figure 8: Experimental arrangement.

used to perform the calibration. These data are supposed to be corrupted by white noise, with a rectangular probability density function. This is corroborated later by means of AVAR and MVAR.

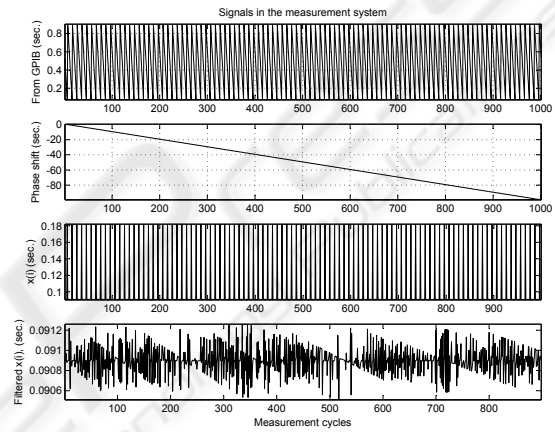


Figure 9: Signals in the measurement chain. From top to bottom: original data from the TIC and the GPIB interface, accumulated phase shift, spiky phase differences, filtered phase differences.

Table 2 summarizes the results of the type B evaluation of the standard uncertainty. It has been reported under the assumption of a rectangular (uniform) probability distribution of the magnitudes X_i (see the factor $\sqrt{3}$ in the particular uncertainties). The rightmost column has been rounded according to the resolution of the TIC.

The expression for the standard uncertainty is obtained from equation 16:

$$u^2(z) = 2 \times \sum_{i=1}^N u_i^2(z) + VAR, \quad (16)$$

where the double factor is due to the fact that we are measuring phase differences. Type A uncertainty (VAR) have been included, resulting $2 \times 10^{-4} s$. The expanded uncertainty of the measurement is stated as the standard uncertainty multiplied by the coverage factor $k=2$, which for a normal distribution attributed to the measurand corresponds to a coverage probability of approximately 0.95. The reported result of the measurement is $f_{meas} = 1.0974 \pm 0.0004 Hz$, for a total measurement time of 898 s.

Table 2: Sources of the type B uncertainty assuming white noise (TIC HM8122). Top to bottom: X_1 (± 1 ext. clock from GPS receiver), X_2 (Time base error from GPS clock's accuracy), X_3 (Jitter), X_4 (Systematic error), X_5 (Resolution from GPS receiver HM8125), X_6 (Accuracy), X_7 (Jitter), X_8 (Averaging time of the measurement system: $u^2(x_8) = u^2(x_6) + u^2(x_7)$). Units in [ns].

Value	Std. uncertainty $u(x_i)$	Contribution $u_i(z) = c_i \times u(x_i)$
100	$\frac{100}{\sqrt{3}}$	70
100	$\frac{100}{\sqrt{3}}$	70
5	$\frac{5}{\sqrt{3}}$	4
< 4	$\frac{4}{\sqrt{3}}$	3
100	$\frac{50}{\sqrt{3}}$	4
100	$\frac{100}{\sqrt{3}}$	70
5	$\frac{5}{\sqrt{3}}$	4
6	6	0.5

4.2 Testing for White Noise

The ratio of the classical variance (VAR) to the Allan variance (AVAR) provides a primary test for white noise. This quantity (0.672) is less than $1 + 1/\sqrt{m} \approx 1.033$; thus it is probably safe to assume that the data set is dominated by white noise, and the classical statistical approach can safely be used. Failure of the test does not necessarily indicate the presence of non-white noise (Fluke, 1994). A slope test (based in AVAR and MVAR curves) has been developed to confirm the presence of white noise. AVAR and MVAR curves are depicted in figure 10.

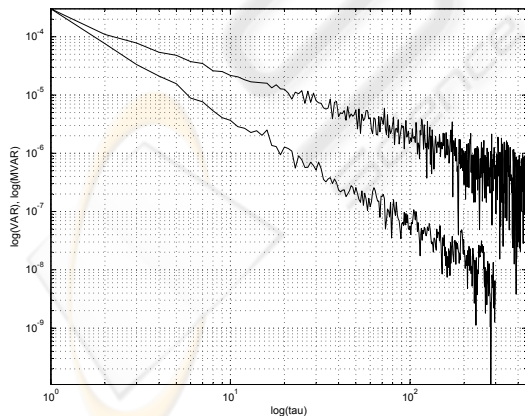


Figure 10: AVAR (upper) and MVAR (lower) log-log curves. The final calibration period is $\tau = 500 \times \tau_0$ for $\tau_0 = 1$ s.

Measures of the slopes over the log-log graphs in figure 10 offer the results -1 and -1.5 for $\log(AVAR)$

vs. $\log(\tau)$, and $\log(MVAR)$ vs. $\log(\tau)$, respectively; which indicate that a white phase modulation process is coupled to the frequency source under test (see table 1).

5 CONCLUSION

Frequency calibrations using incomplete data sheets can be performed by means of the white noise hypothesis. This conveys the idea of using uniform probability distributions for which classical variances are easily computed. Since the sensibility coefficients in the expression of the uncertainty of the measurement are computed under this assumption, it has to be corroborated later. Two tests have been revised and applied successfully. The numerical (first) test is in turned corroborated by the slope test. Sources of Type B uncertainty have been calculated considering the white noise assumption.

ACKNOWLEDGEMENTS

The authors would like to thank the *Spanish Ministry of Education and Science* for funding the project DPI2003-00878 which involves noise processes modelling and time-frequency calibration.

REFERENCES

- (1988). IEEE standard definitions of physical quantities for fundamental frequency and time metrology. Technical Report IEEE Std 1139-1988, The Institute of Electrical and Electronics Engineers, Inc., 345 East 47th Street, New York, 10017, USA.
- Allan, D. (1987). Time and frequency (time-domain) characterization, estimation, and prediction of precision clocks and oscillators. *IEEE Transactions on Ultrasonics, Ferroelectrics, and Frequency Control*, 34(752):647–654.
- de la Rosa, J. J. G., Galiana, I. L., Puntonet, C. G., and López, V. P. (2005). A graphical review of noise-instability characterization in electronic systems. In *Proceedings of ICINCO 2005 Second International Conference on Informatics in Control*, volume 3, pages 11–18, Hosted by Escola Superior de Tecnologia de Setúbal, Portugal. ISBN 972-8865-12-0 Institute for systems and Technologies of Information Control and Communication (INSTICC Press). Paper 50 in Signal Processing, System Modeling and Control (Poster).
- Fluke (1994). *Calibration: Philosophy in Practice*. Fluke, 2 edition.

- Force, E. T. (1999). *Expression of the uncertainty of measurement in calibration EA-4/02*. EA European cooperation for Accreditation (ISO).
- Greenhall, C. (1988). Frequency stability review. TDA progress report. Technical Report 42-88, Communications Systems Research Section.
- Howe, D., Allan, D., and Barnes, J. (1999). Properties of oscillator signals and measurement methods. Technical report, Time and Frequency Division. National Institute of Standards and Technology.
- Lesage, P. and Ayi, T. (1984). Characterisation of frequency stability: Analysis of the modified allan variance and properties of its estimate. *IEEE Trans. on Instrumentation and Measurement*, IM-33(4):332–336.
- Lombardi, M. (1996). An introduction to frequency calibrations. *The International Journal of Metrology*, (January/February 1996).
- Rutman, J. and Walls, F. (1991). Characterization of frequency stability in precision frequency sources. *Proc. IEEE*, 79(7):952–960.
- Vernotte (1993). Oscillator noise analysis: Multivariate measurement. *IEEE Transactions on Instrumentation and Measurement*, 42(2):342–350.
- Vig, J. R. (2001). *A Tutorial For Frequency Control and Timing Applications*.



SciTeP Press
Science and Technology Publications